

Faraday Effect

Muhammad Shairil Danil Bin Sidin

A0182458W

Abstract

In this experiment, we determined the angle of rotation of the polarization-plane of the polarized light through a flint glass rod as a function of the mean-flux density using different colored filters, calculate their corresponding Verdet's constant in each case as well as evaluate Verdet's constant as a function of the wavelength and the optical medium. We were able to obtain an experimental value of Verdet's constant to be $(34.0 \pm 2.7) \text{ rad m}^{-1}\text{T}^{-1}$, $(62.3 \pm 4.6) \text{ rad m}^{-1}\text{T}^{-1}$, $(51.7 \pm 8.1) \text{ rad m}^{-1}\text{T}^{-1}$, $(43.3 \pm 2.5) \text{ rad m}^{-1}\text{T}^{-1}$ and $(39.6 \pm 1.8) \text{ rad m}^{-1}\text{T}^{-1}$ correspondingly for colored lenses of 440nm, 505nm, 525nm, 580nm and 595nm. Similarly, the theoretical values of the Verdet's constants are $49.5 \text{ rad m}^{-1}\text{T}^{-1}$, $34.2 \text{ rad m}^{-1}\text{T}^{-1}$, $31.1 \text{ rad m}^{-1}\text{T}^{-1}$, $24.5 \text{ rad m}^{-1}\text{T}^{-1}$ and $23.1 \text{ rad m}^{-1}\text{T}^{-1}$. This gives us a percentage discrepancy of 31.4%, 81.8%, 66.3%, 77.2% and 71.8%.

1 Introduction

When a beam of plane-polarized light passes through a transparent medium permeated by an external magnetic field with lines of magnetic force parallel to the direction of incident light, it can be seen that the plane of polarization of light is rotated. The angle of rotation of the plane of polarization is proportional to the length, l , of the distance in which light travels through the test specimen according to the equation:

$$\Delta\theta = V(\lambda) \cdot l \cdot B \quad (1)$$

, where $V(\lambda)$ is the Verdet's constant. A Verdet's constant of $V(\lambda) > 0$ corresponds to an anti-clockwise rotation and diamagnetic materials whereas a Verdet's constant of $V(\lambda) < 0$ corresponds to a clockwise rotation and paramagnetic materials.

Verdet's constant as a function of the wavelength can be represented by the following empirical expression:

$$V(\lambda) = \frac{\pi}{\lambda} \cdot \frac{n^2(\lambda) - 1}{n(\lambda)} \cdot \left(A + \frac{B}{\lambda^2 - \lambda_0} \right) \quad (2)$$

, where the refractive index $n(\lambda)$ can be calculated using:

$$n(\lambda) = \sqrt{1 + \sum_{i=1}^3 \frac{B_i \lambda^2}{\lambda^2 - C_i}} \quad (3)$$

A , B , B_i and C_i are constants and their values are shown below:

$$\begin{aligned} A &= 15.7116\text{E}-7 \text{ rad/T} \\ B &= 6.3430\text{E}-19 \text{ m}^2\text{rad/T} \\ \lambda_0 &= 156.4 \text{ nm} \\ B_1 &= 1.72448482 \\ B_2 &= 0.390104889 \\ B_3 &= 1.04572858 \\ C_1 &= 0.0134871947 \text{ }\mu\text{m}^2 \\ C_2 &= 0.0569318095 \text{ }\mu\text{m}^2 \\ C_3 &= 118.557185 \text{ }\mu\text{m}^2 \end{aligned}$$

2 Experiment

- 1) Condenser, $f=6\text{cm}$
- 2) Coloured glass
- 3) Polarizer
- 4) Test specimen (flint glass SF6)
- 5) Analyzer
- 6) Lens, $f=15\text{cm}$
- 7) Translucent screen

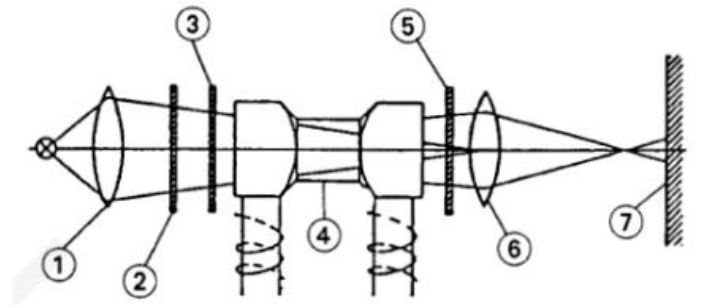


Figure 1: Diagram of the Experimental setup

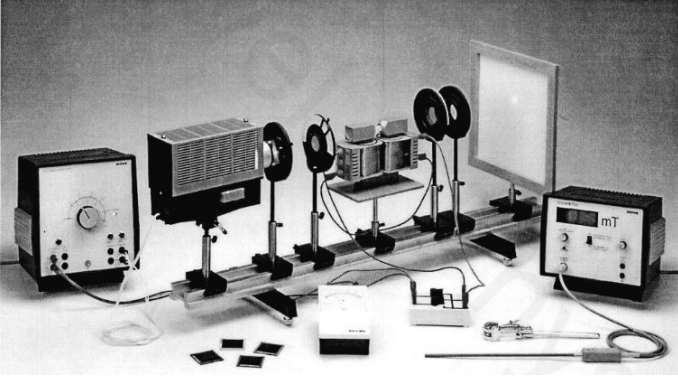


Figure 2: Picture of Experimental setup

The experiment was set-up as per the image above. By inserting varying colored glasses ranging from 440nm to 595nm into the diaphragm holder (labelled (2) as seen from Fig 1), we can obtain various extinction values for each of these glasses. The extinction value is obtained when the light upon the screen is at its dimmest. The angle in which the analyzer was rotated by to reach perfect extinction level is recorded while the polarizing filter is fixed at a permanent position 90° . Note that the 30mm flint glass rod is aligned to the optical axis.

Plane-polarized light is passed through a flint-glass SF6 cylinder, supported between the drilled pole pieces of an electromagnet. An analyzer arranged beyond the glass cylinder has its polarization plane crossed in relation to that of the polarizer, so that the field of view of the face of the glass cylinder projected on the translucent screen appears dark.

By varying the current flowing through the coils of the electromagnets, we can vary the magnetic flux density in between the two pole pieces, and therefore, change the angle of rotation required by the analyzer to achieve best extinction. The values of the current is read of a digital multimeter while the magnetic field was obtained from the graph provided.

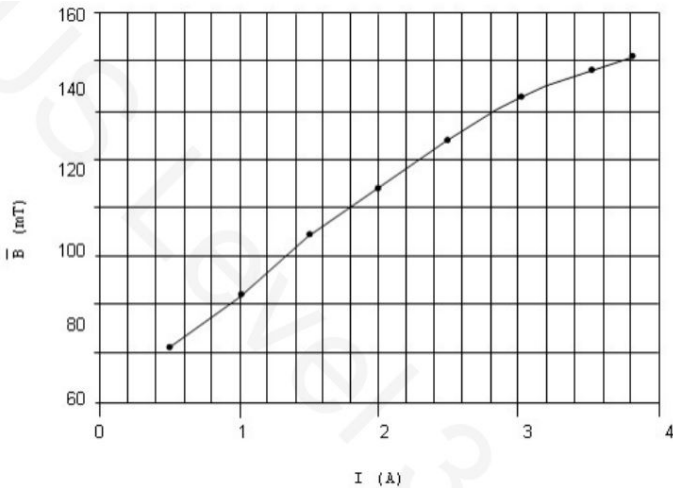


Figure 3: Mean-flux density between the pole pieces as a function of the coil current.

The corresponding mean-flux density was obtained for each current values:

Current (± 0.082 A)	Mean-flux Density (± 0.16 mT)
0.500	80.90
1.000	91.80
1.500	104.50
2.000	114.00
2.500	124.00
3.000	133.10

3 Results & Analysis

Following the procedures as described above, we were able to get the experimental values of Verdet's constant to be $(34.0 \pm 2.7) \text{ rad m}^{-1}\text{T}^{-1}$, $(62.3 \pm 4.6) \text{ rad m}^{-1}\text{T}^{-1}$, $(51.7 \pm 8.1) \text{ rad m}^{-1}\text{T}^{-1}$, $(43.3 \pm 2.5) \text{ rad m}^{-1}\text{T}^{-1}$ and $(39.6 \pm 1.8) \text{ rad m}^{-1}\text{T}^{-1}$ correspondingly for colored lenses of 440nm, 505nm, 525nm 580nm and 595nm. These values were obtained using the gradient of the graphs between twice the angle of rotation and the mean-flux density. Verdet's constant, $V(\lambda)$, is obtained using the equation:

$$V(\lambda) = \frac{\Delta\theta}{l \cdot B} \quad (4)$$

, where l is 30mm. We plotted $2\Delta\theta$ of the various wavelengths against mean-flux density as can be seen below.

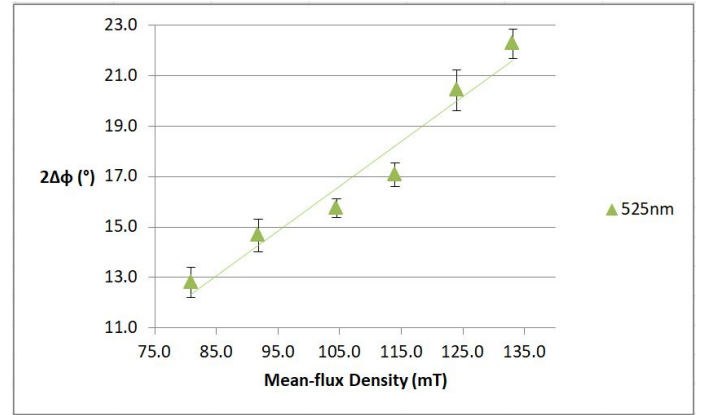


Figure 4: Graph of $2\Delta\theta$ against Mean-Flux Density for 525nm wavelength. Similar graphs for the other wavelengths and comparison among the wavelengths can be found in the Appendix.

Therefore, we were then able to obtain the various Verdet's constant and plot them against the wavelength, as can be seen in Fig. 5. Aside from the Verdet's constant obtain for 440nm wavelength, the Verdet's constant decreases as the wavelength increases.

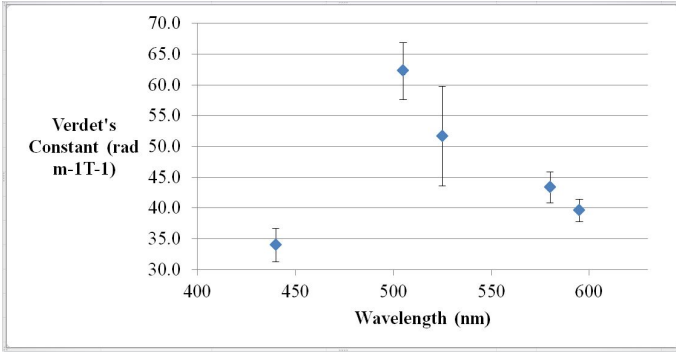


Figure 5: Graph of Verdet's constant against wavelength.

The following table depicts the Verdet's constant in different units; degree and radians.

Wavelength	$V(\lambda)$ ($^{\circ}/\text{Tm}$)	$V(\lambda)$ (rad/Tm)	Uncertainty (rad/Tm)
440	1946.7	34.0	2.7
505	3566.7	62.3	4.6
525	2960.0	51.7	8.1
580	2483.3	43.3	2.5
595	2270.0	39.6	1.8

Figure 6: Table of wavelength against Verdet's constant in different units.

Meanwhile, the theoretical values were calculated using Eqn. (2), (3) as well as the table proceeding that. We also checked the values calculated against the database from refractiveindex.info. The theoretical values are shown below:

Wavelength	Theoretical Value of $V(\lambda)$ (rad/Tm)
440	49.5
505	34.2
525	31.1
580	24.5
595	23.1

Figure 7: Table of wavelength against theoretical Verdet's constant.

By comparing our experimental Verdet's constant values against the theoretical values, we were able to get a percentage discrepancy correspondingly for each wavelength to be 31.4%, 81.8%, 66.3%, 77.2% and 71.8%. The graph below depicts the graph for the theoretical and experimental Verdet's constant. As mentioned, there is a large discrepancy and an anomalous point for 440nm.

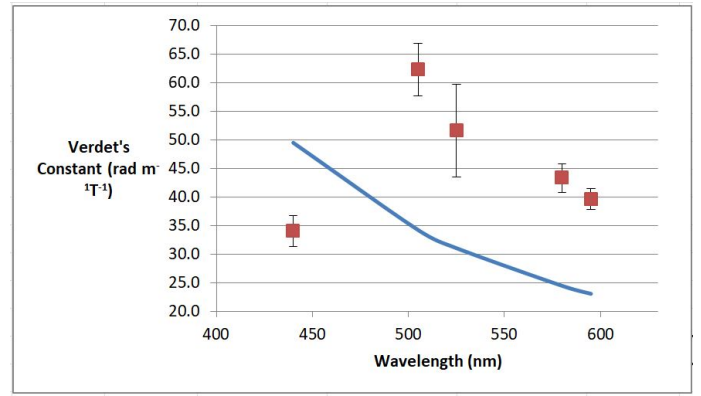


Figure 8: Graph of the theoretical and experimental Verdet's constant against wavelength.

4 Discussion

A. Anomalous point for 440nm

The Verdet's constant for 440nm deviates the most from the general trend as it is most likely due to the fact that the light shone on the screen is extremely dim at that level. As so, it is difficult to determine when the extinction point has been achieved. Due to the single digit range of angle of rotation, a slight adjustment to the analyzer will result in a change in the angle of rotation. While this change is usually about at most 1° , it has a large effect on the Verdet's constant.

B. Large percentage discrepancy

The large percentage discrepancy is due to several factors. Firstly, we were not able to measure the value of the mean-flux density between the pole pieces as there was no probe to measure with. As so, we had to obtain our values of mean-flux density from the graph. The analog reading, not only does it add uncertainty to our values, but are also hard to determine as the points seems to be shifted from the grid lines as well as the fact that the values of current that we are required to use are not the points that were plotted on the graph.

Additionally, we had to determine the extinction by sight. This is extremely unreliable as it is difficult to ascertain when the dimmest point on the screen has been achieved.

Lastly, the current running through the coils for the electromagnets varies against time due to heating of the coils. As so, the mean-flux density between the two pole pieces varies while attempting to determine the extinction points. However, as the mean-flux density and current has changed during the measurements, the values recorded might vary from what was initially expected. While the current might change by around 0.1A, the extremely small values of mean-flux density we are operating within (militesla) causes a significant deviation on the angle of rotation of the analyzer recorded.

C. Suggestions on improving the experiment

Firstly, the experiment can be isolated further. While efforts were made to ensure that there were not any stray light around when recording the extinction point for the light upon the screen, it was difficult to achieve complete darkness when another experiment was being conducted at the table beside. The stray light made it difficult to ascertain the extinction point and causes the angle of rotation recorded to be inaccurate. Thus, it is suggested that only one experiment be conducted within each curtained zones.

Another suggestion is to provide us with a probe so that we may measure the mean-flux density between the pole pieces. This allows us to get a more accurate reading instead of relying on the analog graph.

Lastly, a photometer would be crucial in determining the extinction point. Using a digital instrument, would not only reduce the uncertainty in reading, but also allow us to determine accurately when the dimmest point has been achieved. Furthermore, it speeds up data recording as it is much easier to read off a digital reading then trying to determine the analog analyzer.

5 Conclusion

We were able to obtain an experimental value of Verdet's constant to be $(34.0 \pm 2.7) \text{ rad m}^{-1}\text{T}^{-1}$, $(62.3 \pm 4.6) \text{ rad m}^{-1}\text{T}^{-1}$, $(51.7 \pm 8.1) \text{ rad m}^{-1}\text{T}^{-1}$, $(43.3 \pm 2.5) \text{ rad m}^{-1}\text{T}^{-1}$ and $(39.6 \pm 1.8) \text{ rad m}^{-1}\text{T}^{-1}$ correspondingly for colored lenses of 440nm, 505nm, 525nm 580nm and 595nm. Similarly, the theoretical values of the Verdet's constants are $49.5 \text{ rad m}^{-1}\text{T}^{-1}$, $34.2 \text{ rad m}^{-1}\text{T}^{-1}$, $31.1 \text{ rad m}^{-1}\text{T}^{-1}$, $24.5 \text{ rad m}^{-1}\text{T}^{-1}$ and $23.1 \text{ rad m}^{-1}\text{T}^{-1}$. This gives us a percentage discrepancy of 31.4%, 81.8%, 66.3%, 77.2% and 71.8%. We proved the linear relationship of between the angle of rotation and Mean-flux density, the proportionality factor, also known as the Verdet's constant, $V(\lambda)$, its relationship with varying wavelength as well as sources of errors and ways to improve the experiment.

6 References

[1]: Kheamrutai Thamaphat, Piyyarat Bharmanee, and Pichet Limsuwan. *Measurement of verdet constant in diamagnetic glass using faraday effect*. Editorial Board: Natural Sciences Social Sciences, Kasetsart University, Bangkok, Thailand, page 18, 2006.

[2]: Sellmeier's coefficients for sf6. URL <https://refractiveindex.info/?shelf=glassbook=>

[3]: Martinez, L., F. Cecelja and R. Rakowski. 2005. *A Novel Magneto-optic Ferrofluid Material for Sensor Applications*. *Sensors and Actuators A*. 123-124: 438-443.

[4]: Ruan, Y., R.A. Jarvis, A.V. Rode, S. Madden and B.L. Davies. 2005. *Wavelength Dispersion of Verdet Constants in Chalcogenide Glasses for Magneto-optical Waveguide Devices*. *Optics Communications* 252: 39-45

[5]: Udd, E. 1991. *Fiber Optic Sensors: An Introduction for Engineers and Scientists*. John Wiley Sons, Inc., New York.

[6]: Weber, M.J. 1995. *CRC Handbook of Laser Science and Technology*. Vol. V. Part 3. CRC Press, Boca Raton.

[7]: Williams, P.A., A.H. Rose, G.W. Day, T.E. Milner and M.N. Deeter. 1991. *Temperature Dependence of The Verdet Constant in Several Diamagnetic Glasses*. *Applied Optics* 30: 1176-1178.

[8]: Zvezdin, A.K. and V.A. Kotov. 1997. *Modern Magneto-optics and Magneto-optical Materials*. Institute of Physics Publishing, Bristol.

7 Appendix

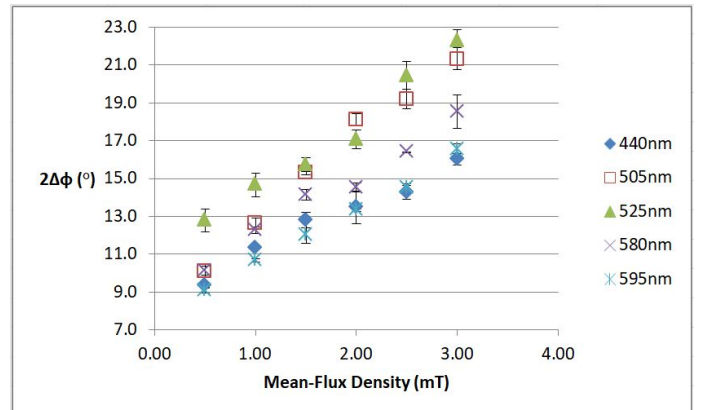


Figure 9: Graph of $2\Delta\theta$ against Mean-Flux Density for the various wavelengths.

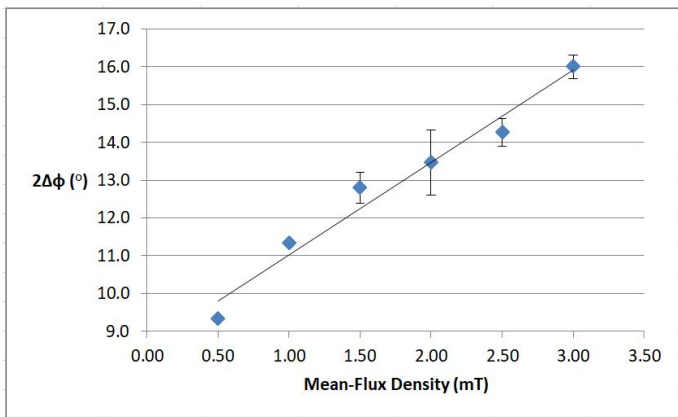


Figure 10: Graph of $2\Delta\theta$ against Mean-Flux Density for 440nm wavelengths.

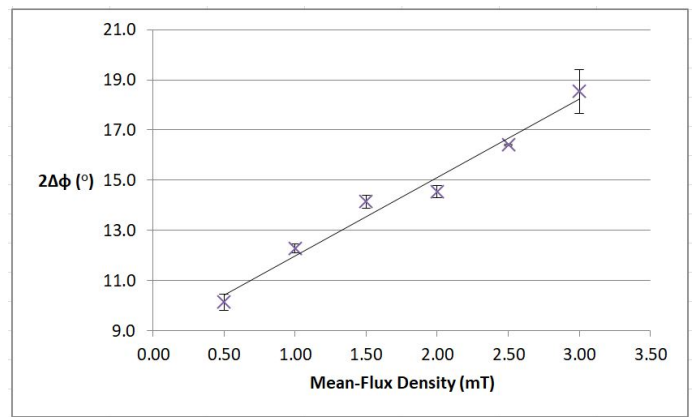


Figure 12: Graph of $2\Delta\theta$ against Mean-Flux Density for 525nm wavelengths.

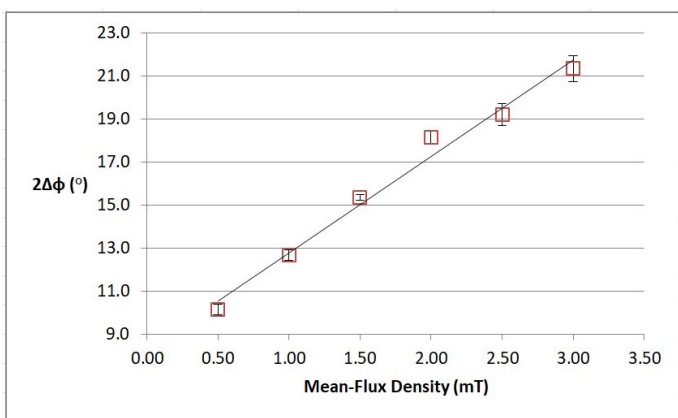


Figure 11: Graph of $2\Delta\theta$ against Mean-Flux Density for 505nm wavelengths.

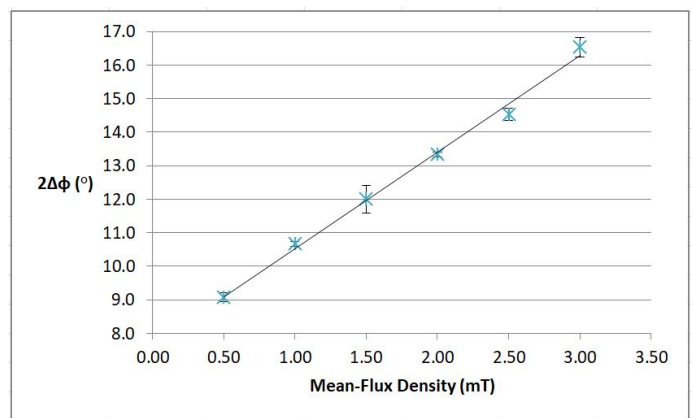


Figure 13: Graph of $2\Delta\theta$ against Mean-Flux Density for 595nm wavelengths.